Effect of pressure on the resonant multiphonon Raman scattering in UO_2

Tsachi Livneh* and Eran Sterer
Nuclear Research Center, Negev, P.O. Box 9001, Beer-Sheva, 84190 Israel
(Received 21 November 2005; published 28 February 2006)

The phonon Raman scattering in UO_2 was investigated under pressures up to 29 GPa with the excitation energy range of $E_i = 1.16-2.41$ eV. At ambient pressure up to the sixth order polarized multi LO-phonon bands are detected with a resonant profile that follows the UO_2 absorption (threshold of ~2.0 eV). The 1150 cm^{-1} band is reassigned to the 2 LO band rather than to the Γ_5-Γ_3 crystal field electronic transition. The resonance profile of the 1–6 LO intensities is likely to be attributed to a "forbidden" Fröhlich LO(Γ) scattering. However, identification with this form of scattering cannot explain the different polarization sensitivity between the even (strongly polarized) and odd (weakly polarized) bands. Hence, the significant contribution of nearly degenerate disorder induced phonons, extending over the Brillouin zone from Γ to L boundaries, is suggested. Three factors are mainly responsible for the pressure dependent behavior of the 1 LO and 2 LO bands: (i) A redshift in the resonance onset, which is related to the decrease in the band gap energy, (ii) an increase in the relative intensities of the bands, that is due to the increase in electron-phonon interactions, and (iii) a decrease in the incident and scattered light penetration depth, that is due to the increased absorption. An interplay between the first two (increasing) and the third (decreasing) is dictating the intensity of the LO bands.

DOI: 10.1103/PhysRevB.73.085118 PACS number(s): 78.30.Am, 07.35.+k, 62.50.+p

I. INTRODUCTION

Due to its technological and scientific significance, uranium dioxide is one of the most extensively studied actinide compounds, with its spectroscopic aspects elaborately reviewed by Schoenes.[1,2] UO_2 crystallizes in a fluorite (CaF_2) (space group O_h^5) type structure, where the uranium U^{+4} ions occupy the fcc (face center cubic) sites and the oxygen O^{-2} ions occupy the tetrahedral sites. Three frequencies are detected around the center of the Brillouin zone at 278,[1] 445,[3,4] and 578 cm^{-1},[1] were attributed to the doubly degenerate F_{1u} IR active TO mode, triply degenerate F_{2g} Raman active mode, and a nondegenerate F_{1u} IR active LO mode, respectively. A good agreement was found with Brillouin zone center frequencies of UO_2, as measured by inelastic neutron scattering (INS).[5]

Unlike the straightforward assignment of the F_{2g} Raman active mode, the assignment of an additional band at 1150 cm^{-1}, found by Schoenes (at 1145 cm^{-1}) (Ref. 2) is more ambiguous: It was assigned to the Γ_5-Γ_3 electronic Raman crystal field (CF) transition, based on the calculation of the parameters that construct the CF Hamiltonian made by Rahman and Runciman.[6] Although INS studies[7–9] showed the predominant $^3H_4$ CF levels to be in discrepancy with the calculated ones, the assignment of the 1150 cm^{-1} band[2] remained unchanged in the following Raman studies of UO_2.[4,10–13] This is mostly due to the accepted notion that a decrease in intensity with temperature [$I_{300\ K} \approx 0.25\ I_{20\ K}$ for UO_2 (Refs. 2,12)] is not expected from pure multiphonon excitation but rather from a band of electronic origin.

Various groups studied the structural properties of UO_2 under high hydrostatic pressures.[14–20] These studies showed that similar to CeO_2 (Ref. 21) and ThO_2,[20,22] UO_2 undergoes a CaF_2-type$\rightarrow$$PbCl_2$-type structural phase transition. This transition does not involve 5*f* electrons delocalization.[23] According to the most recent study that extended to 69 GPa the high pressure phase appears in UO_2 at ~42 GPa,[20] relative to 31 and 35 GPa for CeO_2 (Ref. 21) and ThO_2,[20] respectively. Polarized and pressure dependent Raman scattering was studied for CeO_2 (Refs. 24,25) and ThO_2.[26,27] For both compounds the phonon dispersion curves were calculated and the two phonon densities of states (DOS) were constructed.

UO_2 in its ground state is not a conventional semiconductor, but rather a Mott insulator—an insulator that is characterized by the existence of localized electrons, each cation having the configuration U^{+4} ($5f^2$).[28–30] The predominance of repulsive Coulomb interaction between the two 5*f* electrons lead to the creation of semiconductor carriers. The altered-valency (U^{+3}) and (U^{+5}) cations that are formed require the expenditure of energy U (Mott-Hubbard gap).[29] In the absence of further interactions the electrons (U^{+3}) and holes (U^{+5}) will be free to move. However, in the case of UO_2 a strong interaction of the electrons with the LO phonons destroy the extended nature of the charge carrier states. Electrons are localized in small-polaron eigenstates[28–30] and their movement is accompanied by displacements of the ions around them while carrying along the lattice deformation. Being accompanied by the much heavier lattice degrees of freedom in the polaronic regime the carriers acquire large effective masses. The mechanism of polaron formation enhances phonon assisted optical transitions in the range of energies below the band gap with a transition probability that is related to the distribution of the LO phonons.[30] Static displacement of the normal coordinates of the $\mathbf{k} \sim 0$ phonons may also be produced by localized excitations that couple strongly to the lattice through the Fröhlich interactions.[31] Such displacements give rise to Franck-Condon terms that can produce multiphonon scattering near resonance and must vanish away from resonance, as was shown for YbS that are characterized by 4*f* localization.[32] It is, therefore, our objective to search for the "forbidden" mul-

tiphonon LO(Γ) resonance Raman scattering for the UO_2, a system that is characterized by $5f$ localization.

Optical spectroscopy was shown to be highly valuable in revealing the role played by the $5f^2$ band at ambient conditions.[1,2] The complexity of its absorption spectra[1,33] is reflecting the importance in the $5f$ electronic system of crystal field effects and spin orbit splitting, both in the eV energy regime. Optical reflectivity measured between 0.5 and 3.5 eV revealed[15–17] that at pressures above ~15 GPa a number of narrow optical transitions at energies between 0.5 and 2eV become observable, attributed to transitions within the $5f^2$ multiplet levels of UO_2. The increasing strength of these normally dipole forbidden excitations was suggested to indicate an increasing admixture of presumably d-like character to the $5f^2$ configuration.

Recently, the electronic structure of UO_2 has been calculated by the hybrid density functional theory (DFT) (Ref. 34) and good agreement was found with the experimental gap, DOS, and optimum lattice constant. The picture emerging from the hybrid calculations is different from that of Schoenes[1] who associated the gap with $5f \rightarrow 6d$ transitions and localized $5f \rightarrow 5f$ transitions lying in the gap. Rather, the band at the Fermi level, E_f, is dominantly of a $5f$ nature, in agreement with a resonant photoemission study.[35] The unoccupied DOS appears consistent with optical spectra and the levels at the onset of the conduction band are composed of unoccupied f states, meaning that the gap is composed from $5f \rightarrow 5f$ transitions.

In this paper we investigate the phonon polarized Raman scattering in UO_2 with an excitation energy range 1.16–2.41 eV at pressures up to 29 GPa. We show that the 576 cm^{-1} band is a resonantly enhanced LO scattering. This band is activated up to its sixth order with the 1150 cm^{-1} band being its first overtone. We show that the pressure induced redshift in the absorption threshold "tunes" the resonance behavior as manifested in the intensities of the LO band and its first overtone.

II. EXPERIMENT

The UO_2 sample was synthesized by the sintering of UO_2 powder in a hydrogen flow at 1700 °C.[36] Electrochemical polishing of the pellet was followed by X-ray diffraction (XRD) measurements in order to verify the good structural quality of the sample. The pellet is constructed from ~20 μm single crystals with various (unidentified) crystallographic orientations. Backscattering geometry Raman measurements were obtained from a Renishaw dispersive spectrometer by using an objective of ×100 (NA=0.9) (NA—numerical aperture) at three excitation wavelengths of 782, 632.8, and 514.5 nm, that correspond to excitation energies of 1.58, 1.96, and 2.41 eV, respectively. For the 1064 nm excitation wavelength (1.16 eV) a Bruker Fourier-transform (FT)-Raman spectrometer was used. The polarization of the incident light could be either parallel **Ei**∥**Es**, or perpendicular **Ei** ⊥ **Es** to the scattering plane by placing a λ/2 plate in the p-polarized incident laser beam before it reached the sample. A polarizer that was placed in the scattered beam path ensured the detection of the light scattered parallel to the scattering plane.

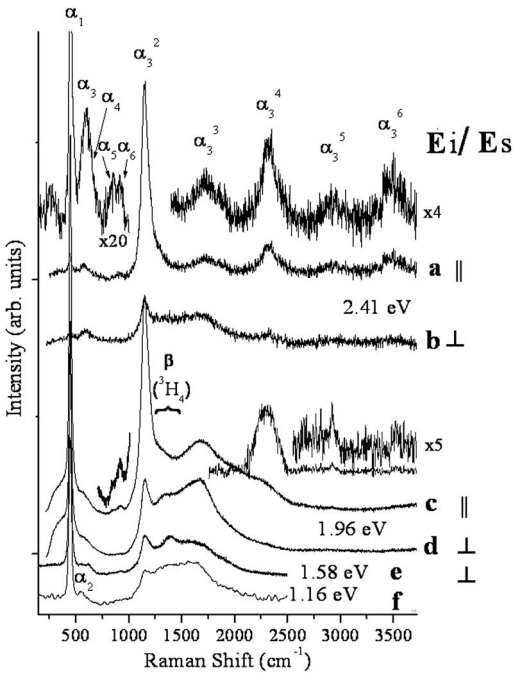

FIG. 1. The Raman spectrum of UO_2 measured under ambient conditions for an excitation energy range of E_i=1.16–2.41 eV, with the denoted **Ei**∥**Es** and **Ei** ⊥ **Es** polarization configurations. All bands are assigned in accordance with Table I (a) and (b) E_i =2.41 eV in the **Ei**∥**Es** and **Ei** ⊥ **Es** polarization configurations, respectively. (c) and (d) E_i=1.96 eV in the **Ei**∥**Es** and **Ei** ⊥ **Es** polarization configurations, respectively, with the α_3^4-α_3^6 bands shown after subtraction of adjacent overlapping bands. (e) E_i=1.58 eV in the **Ei** ⊥ **Es** polarization configuration. (f) Unpolarized FT-Raman spectrum with E_i=1.16 eV.

In the pressure dependent measurements a 30 μm grain was inserted in a Tel-Aviv-type diamond anvil cell[37] with solid Ar serving as a pressure transmitting medium without allowing the bridging of the sample between diamond anvils. The culet diameter was 500 μm and a stainless steal gasket was used. The Pressure was measured by the Ruby luminescence method.[38] Backscattering geometry Raman measurements were done by using a ×40 long focal length objective.

III. RESULTS AND DISCUSSIONS

A. Band assignments and their Grüneisen parameters

Figure 1 shows the Raman spectrum of UO_2 in the 100–3600 cm^{-1} range, measured under ambient conditions for an excitation energy of E_i=1.16–2.41 eV in the denoted polarization configurations. Up to 1000 cm^{-1} six phonon bands are observed at 445(α_1), ~550(α_2), 576(α_3), 630(α_4), 835(α_5), and 918 cm^{-1}(α_6). The α_1 band is the Raman allowed first-order mode with F_{2g} symmetry.[3,4] A strong band is also observed at 1150 cm^{-1}. This band is attributed to an overtone of the α_3 (α_3^2-—as we denote the nth order of the α_m band by $\alpha^n{}_m$). In fact, as is clearly observed in Figs. 1(a) and 1(b) (E_i=2.41 eV) the bands at 576 and 1150 cm^{-1} are actually the first two from a consecutive series of six bands at 576(α_3), 1150(α_3^2), ~1725(α_3^3), 2312(α_3^4), 2910(α_3^5),

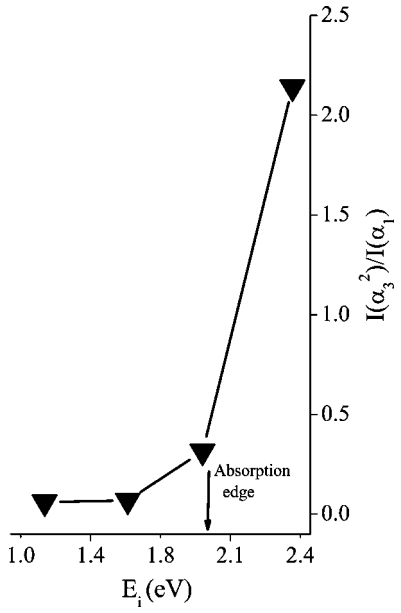

FIG. 2. The intensity ratio between the unpolarized α_3^2 (2 LO) band and the α_1 (F_{2g} Raman allowed band) for a freshly polished UO_2 sample. The UO_2 absorption edge is shown for reference.

and 3470 cm^{-1}(α_3^6). The α_3 frequency is practically similar to the LO phonons frequency at the Γ enter of Brillouin zone.[1,5] However, as a result of disorder induced effects[4] nearly degenerate phonons extending over the Brillouin zone from Γ to L boundaries may also be found at similar energies, due to the flat dispersion in the $\Lambda_1(01)$ phonon branch.[5]

Finally, in the 1000–2000 cm^{-1} range we additionally observe a series of electronic and electronic-phononic Raman bands that are related with CF states with predominately $^3H_4$ character, as found by INS.[7–9] An elaborate discussion on these bands will be given elsewhere.[39]

While the α_1 band intensity is increased, it is clear that the higher overtones are diminishing as E_i decreases and shifts away from the absorption edge of UO_2($\sim$2.0 eV).[1,33] For E_i=1.96 eV [(c) and (d)], the intensities of the higher $\alpha_3^n(n>2)$ overtones decrease significantly but may still be observed. For E_i=1.16 eV (f), even the 2 LO band is almost vanished (overtones that maintain $\mathbf{k}=0$ may show Raman activity). The above dependence indicates that the activation of the LO series is via a resonance process. A manifestation of this dependence for the α_3^2 2 LO band is shown in Fig. 2, where the intensity of the α_3^2 band (unpolarized) is normalized to the α_1 band, for which we assume to have minor energy dependence on the Raman cross section. Our results are consistent with a recent study[13] for which a single crystal of UO_2 was measured at 1.64 and 2.54 eV.

In order to substantiate our assignment of the 1150 cm^{-1} band to the α_3^2 band, which is different from the assignment of this band to a Γ_5-Γ_3 electronic Raman CF transition,[2,4,10–13] the Raman spectra of UO_2 was measured under hydrostatic pressures up to 29 GPa. Two different UO_2 samples were loaded into an anvil cell: S#1 was measured with E_i=1.96 and 1.58 eV, which are denoted as S#1 (1.96) and S#1 (1.58). S#2 was measured with E_i=1.96 eV at longer acquisition times that enabled the accurate analysis of higher order bands . In Fig. 3 the Raman spectra of UO_2 S#1 (1.96) are shown for pressures up to 20 GPa (a), and S#1 (1.58) up to 27 GPa (b). For clarity of the representation we normalized all the spectra to the α_1 band intensity measured at ambient conditions. Apart from the α_1 band, the α_3 and the α_3^2 dominate the spectra. The similar pressure intensity dependence of the latter two bands is consistent with our attribution. Furthermore, unlike the intensity of the α_1 band, that monotonously decreases with pressure, both α_3 and α_3^2 intensities first increase and than decrease at higher pressures. This behavior is related to pressure induced electronic changes—see the discussion below.

In the inset of Fig. 3 we show the spectra that were acquired from S#2, where the pressure dependence of the 630 cm^{-1}(α_4) and 918 cm^{-1}(α_6) bands are clearly observed. We also monitored an additional band (α_{2a}) and its overtone (α_{2a}^2) that were not observed under ambient conditions, probably due to masking of other bands. Their extrapolated Raman shifts to zero pressure are 515 cm^{-1} and 1040 cm^{-1}, respectively. While the spectral behavior of the α_1 and α_3^2 is similar, a significant decrease in the α_3/α_1 intensity ratio is observed concurrently with the appearance of the α_{2a} band and of another broadband around 850 cm^{-1} (that seems to be constructed from three overlapping bands). Differences between different samples in the nature and abundance of defects that are strongly manifested under high pressures may explain this result. It is also clear that the pressure dependent intensity profile of these two bands is different and that the resonant nature of the α_{2a} band is weaker than that of the α_3 band, although the second-order band of the α_{2a} was also observed at the high pressure range.

The pressure dependent frequencies of the various bands are shown in Fig. 4, for E_i=1.96 eV (S#1 - squares, S#2 - circles) and E_i=1.58 eV (triangles). The corresponding measured mode frequencies ω_o at ambient pressures, their linear pressure coefficients $\partial\omega/\partial P$, and their mode Grüneisen parameters $\gamma=-\partial \ln \omega/\partial \ln V=(B_0/\omega_0)\partial\omega/\partial P$ (where B_0 is the bulk modulus) are shown in Table I.[40] From the three published measurements of bulk modulus that were acquired from XRD data,[14,19,20] we chose the most recent one: 207±2 GPa.[20] The Grüneisen parameters for the α_1 band are found to be $\gamma_{\alpha 1}$=1.28, which is close to that of the CeO_2 and ThO_2 F_{2g} symmetry bands that are calculated to be 1.55 and 1.42, respectively, after using the B_0 values from Refs 41,20 and $\partial\omega/\partial P$ values from Refs. 25,27. As for the α_3 and α_3^2 bands: similarity between $\gamma_{\alpha 3}$=0.52 and $\gamma_{\alpha 32}$=0.55 is consistent with our assignments.

The Grüneisen parameters of the TO modes in ionic crystals were found to be significantly higher than those of the LO modes, in some cases by up to a factor of $\sim$3.[42] For example, the fluorite structures CaF_2 γ_{LO} is significantly lower than that of γ_{TO} with the value of γ_R (2 TO+LO at $\mathbf{k}=0$) lying between the two (γ_{TO}, γ_{LO}, and γ_R are 2.29, 0.78, and 1.83, respectively.[43]) Furthermore, $\gamma_{TO}>\gamma_{LO}$ was also calculated for TO and LO modes that split from the Raman mode as we move away from the Brillouin zone center towards its boundary.[43]

The ratio between γ_{TO} and γ_{LO} for a number of diamond, zinc-blende and wurzite-type structures was shown to increase linearly with the ionicity, as measured by the Szigeti

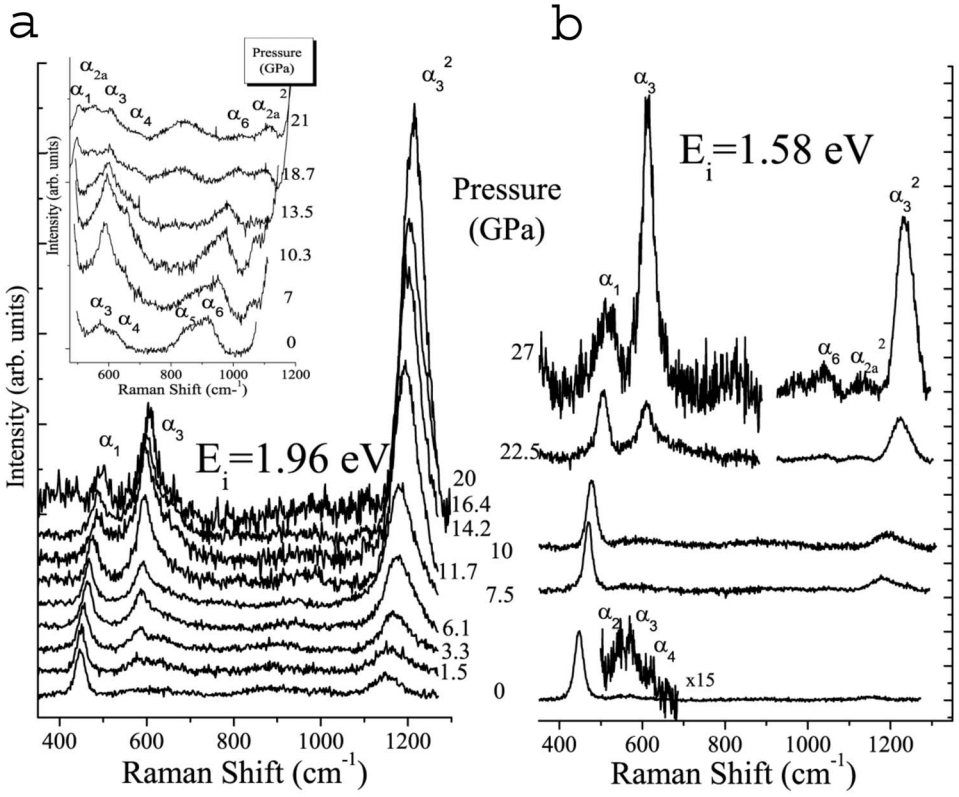

FIG. 3. The Raman spectra of UO_2 from a first sample (S#1) is shown for pressures up to 20 GPa with $E_i=1.96$ eV [S#1 (1.96)] (a) and up to 27 GPa with $E_i=1.58$ eV [S#1 (1.58)] (b). For clarity of representation all spectra are normalized to the α_1 band intensity measured at ambient conditions. In the inset: the spectra acquired from a second sample (S#2) with $E_i=1.96$ eV [S#2(1.96)] at longer acquisition times are shown.

effective charge per cation valence electron, e_s^*/Ze.[42,44] Here $e_s^*=3e^*/(\varepsilon_\infty+2)$ where e^* is Born's transverse dynamic effective charge, and the factor $3/(\varepsilon_\infty+2)$ corrects for the local field due to ion polarizability. The Lyddane-Sahchs-Teller relation yields the following for the ratio of frequencies: $\nu_{LO}/\nu_{TO}=(\varepsilon_0/\varepsilon_\infty)^{1/2}$ (ε_0 and ε_∞ are the low and high frequency dielectric constants, respectively). The decrease in the ν_{LO}/ν_{TO} ratio with the increase in pressure ($\gamma_{TO}\geqslant\gamma_{LO}$) at $\mathbf{k}=0$ was argued[42] to be related to the stiffening of the structure with compression that reduces the relative contribution of ionic displacements to ε_0. Further, the increase of the γ_{TO}/γ_{LO} ratio with an increasing effective charge would follow from the observation that the contribution of ionic motion to ε_0 is relatively more important in compounds having higher ionicity.

The mode Grüneisen parameter of the UO_2 IR active TO mode, γ_{TO} has not been measured but was calculated[45] to be 1.83 by using a repulsive short range potential for rigid ions of the Born-Mayer type (this potential gave reliable consistency with experiments for CaF_2). Other potentials gave higher values but, in general, the trend was reproduced. It is, therefore, concluded that the γ_{TO}, γ_{LO}, and γ_R series for UO_2 of ~1.8, 0.52, and 1.28, respectively, is consistent with what we would generally expect for a crystal with the fluorite structure.[43]

Fluorite-type lattices have nine phonon branches and 45 parity allowed two-phonon combinations and differences modes.[26] Bearing in mind the concept that LO modes should lead to lower γ than the TO modes we shall discuss briefly the assignment of the various phonon bands, as summarized in Table I. The 445 $cm^{-1}(\alpha_1)$ is assigned to the Raman allowed first-order mode with F_{2g} symmetry.[3,4] In the higher energy side of the α_1 band there is a band that is characterized with a profile that is E_i dependent: For $E_i=1.16$ eV [Fig. 1(f)] far from the absorption edge (~2.0 eV),[1] the center of this band is found at ~550 $cm^{-1}(\alpha_2)$. As E_i approaches the absorption edge energy the contribution of another band at 576 $cm^{-1}(\alpha_3)$ increases and obscures the α_2 band. In the

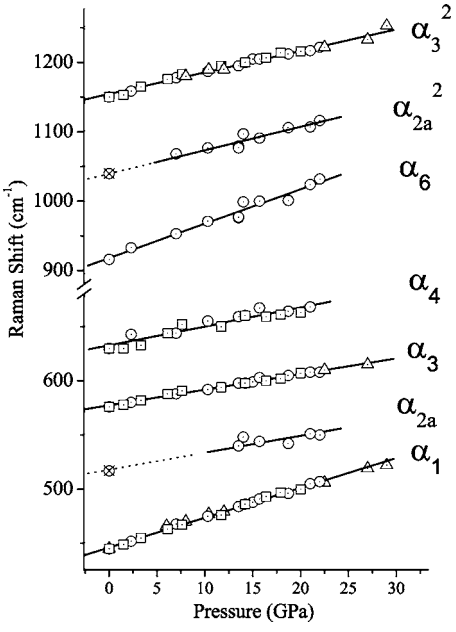

FIG. 4. The pressure dependent frequencies of the various bands for $E_i=1.96$ eV (S#1 - squares; S#2 - circles) and $E_i=1.58$ eV (S#1 - triangles). The Raman shifts of the α_{2a} and α_{2a}^2 were extrapolated to zero pressures.

TABLE I. Assignments and mode Gröneisen parameters of the various bands, using $B_0=207\pm2$. GPa[20].

Band	ω_0 (cm^{-1})	Assignment	$\partial\omega/\partial P$ (cm^{-1}/GPa)	$\gamma=(B_0/\omega_0)\partial\omega/\partial P$
α_1	445	$R(\Gamma)$	2.75 ± 0.04	1.28
α_{2a}	515[a]	?	1.56	0.63
α_2	550	?		
α_3	576	LO[b]	1.45 ± 0.04	0.52
α_4	630	LO (X)	1.73 ± 0.15	0.57
α_5	835	LO(X)+TO(X)?	5.8	
α_6	918	$2TO_R(X)$	4.95 ± 0.30	1.12
${\alpha_{2a}}^2$	1040[a]		3.38 ± 0.24	0.67
${\alpha_3}^2$	1150	2LO	3.08 ± 0.13	0.55
${\alpha_3}^3$	~1725	3LO		
${\alpha_3}^4$	2312	4LO		
${\alpha_3}^5$	2910	5LO		
${\alpha_3}^6$	3470	6LO		

[a]Found only under hydrostatic pressure.
[b]$LO(\Gamma\rightarrow L)$.

lower side of Fig. 3(b) we note that the two bands are observed separately at 1.58 eV. It seems that the assignment of the α_2 and the α_{2a} band at 515 cm^{-1} (not detected under ambient pressure) should be discussed in relation with the high DOS of phonons at this energy range.[5] We suggest that all of these are nearly degenerate phonons with high DOS extending over the Brillouin zone from Γ to L while only the α_3 is being resonance enhanced and therefore more intense at $E_i=2.41$ eV.

As a shoulder to the $\alpha_2+\alpha_3$ band we also observe a band at ~630 $cm^{-1}(\alpha_4)$. This band is dominant on oxidized uranium surfaces and increases in intensity after a heavy ion bombardment of UO_2 polycrystalline surfaces under inert atmosphere.[4] Both heavy ion bombardment and the formation of thin layer of hyperstoichiometric UO_{2+x} on oxidized uranium surfaces (oxygen ions are placed in interstitial sites of the fluorite lattice)[46] will lead to the appearance of new disorder induced bands due to the breakdown of translational symmetry. A possible assignment for the α_4 band is a parity allowed combination of $LO_R(X)+TO_R(X)$. However, the observed Gruneisen parameter $\gamma_{\alpha4}=0.57$ makes it more likely to be a LO phonon. According to Ref. 5 these phonons may originate near the X Brillouin zone edge. We therefore assign the α_4 band to the $LO(X)$ phonon.

Another broad band α_5 is found centered at 835 cm^{-1}. According to the phonon dispersion curves of UO_2 (Ref. 5) various contributions are possible: $2\,LO_R(L)$, $2\,TO_R(L)$, $TO(\Gamma)+LO(\Gamma)$, and $LO(X)+TO(X)$. It is, therefore, difficult to separate the various contributions and our attempt to do so under hydrostatic pressure was not successful. Finally, we assign the α_6 band at 918 cm^{-1} to $2\,TO_R(X)$, which is also consistent with the high polarization sensitivity of this band.

B. The nature of the $\alpha_3{}^n$ bands

It is often that UO_2 with its $5f$ electron localization is compared in the literature to the divalent rare-earth monochalcogenides systems, that are characterized by $4f$ localization.[47] A feature that is commonly found for the latter is the appearance of resonance Raman scattering of the $LO(\Gamma)$ phonon and its overtones. For YbX (X=S, Se, Te) Vitins[48] used a modified version of the "cascade model" in order to account for the multiphonon process. In a later study on YbS Merlin *et al.*[32] employed the configuration-coordinate model, which is based on the Franck-Condon principle in the molecular spectroscopy, where it is assumed that the phonon wave function in the excited state is obtained from that of the ground state after some displacing of the coordinate. By the diagonalization of the phonon Hamiltonian plus the Fröhlich electron-phonon interactions one can obtain polaron states, and the displacement of the phonon in the excited state can be calculated.

A most important result for the 1 LO and 2 LO YbS bands is that the observed decrease in the intensity with an increase of the temperature is due to *lifetime effects of the excited electronic state*. In the explicit formulation of the effective "displacement," the same set of parameters fits the resonance of the 1 LO and 2 LO for a given temperature and only the linewidth has been changed in going from 77 to 300 K [see Eq. (12) in Ref. 32]. A similar approach may be successfully applied to UO_2 and will explain the temperature dependent intensity of the ${\alpha_3}^2$ band.[2,12] Finally, it is important to note, that other examples are known from the literature from which a decrease was observed in the phononic Raman scattering signal with temperature.[49,50]

Another effect in such a scheme is that around resonance the polarization selection rules are expected to be independent of crystal symmetry[31,51] with the maximal intensity for **Ei**$\parallel$**Es**. However, we bear in mind that the treatment that explains polarized scattering usually observed in the multiphonon case depends on the absence of dephasing scattering mechanisms other than LO-phonon scattering in the intermediate state (such as impurity scattering).[31] In Fig. 1 the polarized spectrum of the 2 LO bands is compared for **Ei**$\parallel$**Es** and **Ei**$\perp$**Es** polarization configurations at E_i that are differently positioned with respect to the absorption edge (~2.0 eV): (i) 1.58 eV (far away), (ii) 1.96 eV (close to), and (iii) 2.41 eV (beyond). The intensity ratios for **Ei**$\parallel$**Es**/**Ei**$\perp$**Es** in these measurements are 1.3, 3, and 7, respectively. A similar trend is also established for the 4 LO band. The fact that minor polarization is also observed far from the absorption edge is explained by the fact that an overtone band will always contain the A_1 symmetry representation.

In Fig. 5 the intensity of the various LO multiphonon bands for $E_i=2.41$ eV, with the **Ei**$\parallel$**Es** and **Ei**$\perp$**Es** polarization configurations is shown. Relative to the odd multiples, the even multiples seem to be more intense and polarized. For the Fröhlich electron-phonon interaction (induced forbidden scattering) we would normally expect that *all* the bands should be highly polarized.

It is therefore suggested that the weaker polarization sensitivity of the odd LO modes, and particularly of the 1 LO mode may be due to the contribution of an impurity-induced mechanism that has a weak polarization sensitivity. An additional scattering mechanism that contributes to the scattering cross section is consistent with the different sensitivity of 1

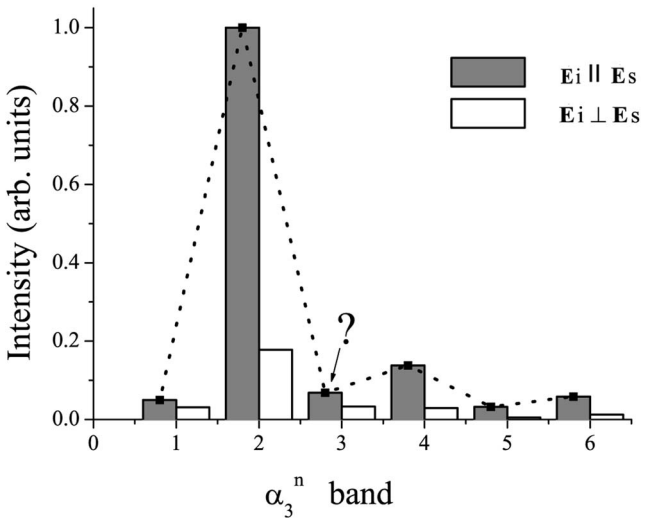

FIG. 5. The intensity of the various α_3^n, $n \leqslant 6$ bands for $E_i = 2.41$ eV, for the **Ei**∥**Es** (gray) and **Ei** ⊥ **Es** (white) polarization configurations. Due to the overlap of the α_3^3 with electronic-phononic Raman bands its intensity is less defined. Relative to the odd multiples, the even multiples are more intense and polarized.

LO and 2 LO to the extent of defects in the lattice; unlike the α_3 band, the α_3^2 band is not highly sensitive to the extent of defects in the UO_2 fluorite structure and does not perturb its translational symmetry.[4] Similar behavior was found for GdS[52] where the defect-induced 1 LO(L) Raman scattering provided a sensitive measure of the sample stoichiometry while the 2 LO(L) was shown to have no defect concentration dependence.

The Yb monochalcogenides do not exhibit only multiphonon light scattering due to zone center LO phonons but also broadband mutiphonon scattering which results primarily from zone-boundary phonons.[48] Multiphonon processes were also observed in magnetic Eu monochalcogenides.[53] In the paramagnetic phase the first-order Raman LO band of these compounds occurs at a frequency of LO(L). This scattering, which does not conserve **k** is due to spin disorder. In the magnetic saturated phase, on the other hand, the spectra show multiphonon scattering at energy multiples of LO(Γ). A major difference between the LO(Γ) and the LO(L) multiphonon scattering is the width of the bands with the latter being much broader than the first.

We conclude that the clear resonance profile of the 1–6 LO intensities is likely to be attributed to ″forbidden″ Fröhlich LO(Γ) scattering. However, an identification with this form of scattering cannot explain the different polarization sensitivity between the even (strongly polarized) and odd (weakly polarized) bands. Probably, disorder-induced effects contribute significantly. However, the phonon dephasing mechanisms that result from these effects are expected to reduce the polarization sensitivity of ″forbidden″ scattering to a much lesser extent than what we observed in our study.[31] It is therefore suggested that a significant role is also played by LO phonons extending over the Brillouin zone from Γ to L boundaries that are nearly degenerate in their energies due to the flat dispersion in the $\Lambda_1(01)$ phonon branch.[5]

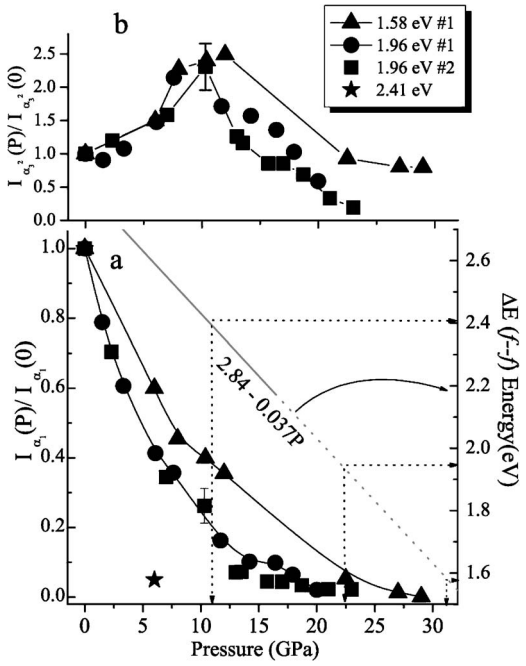

FIG. 6. (a) The intensity of the α_1 band as a function of pressure for the denoted experiments (E_i and # sample). The linear pressure dependence of the reflectivity edge from Ref. 16 is shown with gray solid lines and turns broken at 15 GPa, where the reflectivity edge is no longer observed. Dotted arrows are pointing to the pressure at which E_i intercepts with the line. (b) The intensity of the (α_3^2) band as a function of pressure for the denoted experiments.

C. The pressure induced shift of the resonance Raman onset

In a study that investigated the effect of pressure up to 36 GPa on the optical response of UO_2 a reflectivity edge was identified near 2.8 eV.[15,16] This edge was attributed to the $5f^2 \rightarrow 5f^1 6d_{eg}^1$ excitation (according to the assignment of Schoenes[1,2]). With increasing pressure this transition shifts to lower energy by 37 meV/GPa and its energy roughly corresponds to the energy of the lowest maximum in the imaginary part of the dielectric constant due to the $f \rightarrow d$ transition.[16] Dipole-forbidden excitations within the $5f^2$ multiplet were also observed in the reflectivity spectra above 15 GPa. These transitions were suggested to indicate an increasing admixture of d-like character to the $5f^2$ ground state.

Recently, the electronic structure of UO_2 has been calculated by the hybrid DFT (Ref. 34) and good agreement was found with the experimental gap, density of states, and the optimum lattice constant. We adopt the picture emerging from the calculations that suggests that the onset of the conduction band is composed of unoccupied f states, meaning that the gap is composed from $5f \rightarrow 5f$ transitions *rather* than $5f \rightarrow 6d$ transitions. Consequently, the reflectivity edge near 2.8 eV (Refs. 15,16) should be related to the lowest $5f \rightarrow 5f$ transitions and its pressure induced shift is expected to be manifested in the Raman scattering resonance onset that coincides with the absorption edge ($\sim$2.0 eV).[1] Finally, the extent of f-d orbitals admixture under pressure may be clarified by pressure dependent electronic structure calculations.

In Fig. 6(a) the intensity of the α_1 band is shown as a

function of pressure for the three excitation energies, E_i. The linear pressure dependence of the reflectivity edge from Ref. 16 is also shown with a gray solid line. At 15 GPa, where the reflectivity edge is no longer observed due to the appearance of additional transitions within the $5f^2$ multiplet, we switch to a broken line representation. The $5f \rightarrow 5f$ transition shifts with pressure to lower energy and for each of the three excitation energies a dotted arrow is pointing to the pressure where the laser excitation energy reaches the transition energy. A very good correlation is found between the transition edge pressure and the pressure where the α_1 mode disappears due to increased absorption. For $E_i=2.41$ eV we could not detect a signal up to 1300 cm^{-1} already at pressures around 6 GPa. 20 GPa was sufficient for the signal to lose 95% of the initial value for 1.96 and for 1.58 eV and the signal was still detectable around 29 GPa.

As shown in Fig. 6(b), different behavior is found for the $\alpha_3{}^2$ band: Its intensity increases with pressure up to ~10 and ~12 GPa for $E_i=1.96$ eV and $E_i=1.58$ eV, respectively, and then decreases. The increase in intensity, is attributed to closing the band gap that shifts the absorption edge to lower energy and pushes the Raman resonance profile towards lower excitation energies. However, the pressure increase causes a decrease in the penetration depth of the incident and scattered light and consequentially to the decrease in the α_3 and $\alpha_3{}^2$ intensities.

In Fig. 7 the intensity of the α_3 and $\alpha_3{}^2$ bands relative to the α_1 band is shown for the three different measurements [(S#1 (1.96), S#1 (1.58), and S#2 (1.96))]. We consider the α_1 band to apply as an "internal standard" for the enhancement of the α_3 and $\alpha_3{}^2$ bands, since all factors that are related to changes in the optical and electronic properties will be manifested in both.

For S#1 (1.96), S#2 (1.96) we observe that (i) The relative intensities of the α_3 and $\alpha_3{}^2$ bands superlinearly increase up to ~16 GPa and then decrease. The similarity between their profiles is consistent with their assignment to 1 LO and 2 LO bands, respectively. (ii) The effect of pressure on the resonance behavior of the $\alpha_3{}^2$ mode is stronger than for α_3. However, for S#1 (1.96) and S#2 (1.96) $I(\alpha_3{}^2)/I(\alpha_3)$ is 2.4 and 13, respectively, which is probably related to differences in the extent (and possibly the nature) of defected structures in these samples. (iii) The profiles are markedly different for E_i of 1.96 and 1.58 eV; Up to 20 GPa the former is higher than the latter by a factor of 20. However, it is evident that the relative intensity of the latter is still increasing at pressures where the former is no longer detected. It is, therefore, concluded that the observed α_3 and $\alpha_3{}^2$ intensity profiles are dictated by the proximity of E_i to the pressure dependent band gap energy.

For *S#1* (1.58) there is a *singular pressure range* around 16 GPa where the Raman signal was not distinguishable and a two orders of magnitudes increase in the fluorescence background was detected. This behavior disappeared upon increasing the pressure to 22.5 GPa or reducing it to 12 GPa. Throughout the complete pressure range the background is similar for 1.96 and 1.58 eV (apart from the above-mentioned singular point). A closer look into the (rather weak) pressure dependence of the reflectivity spectra,[15,16] reveals that the (normally dipole forbidden) $^3H_4 \rightarrow {}^3H_6$ transition crosses $E_i=1.585$ eV at ~20 GPa. Consequently, the observed fluorescence background for $E_i=1.585$ eV is probably due to a resonance with the dipole forbidden $^3H_4 \rightarrow {}^3H_6$ transition[54] at pressures around 20 GPa, which is tuned off by either decreasing or increasing the pressure. Finally, since the above transition may contain mixing with lower transitions it may be interesting to measure the effect with a higher pressure resolution around 20 GPa.

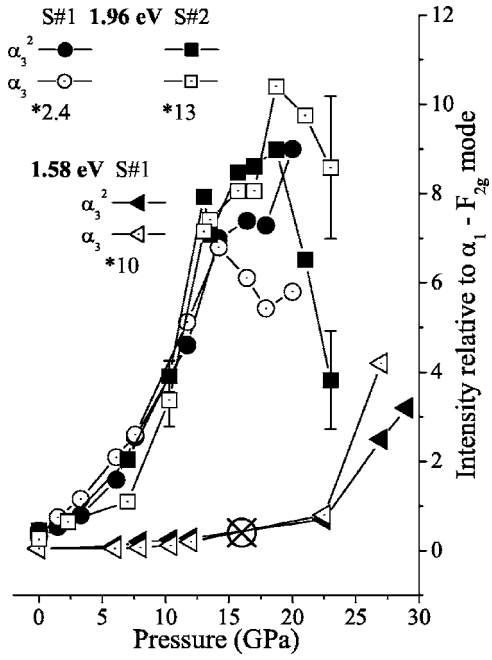

FIG. 7. The intensity of the α_3 (open symbols) and $\alpha_3{}^2$ (filled symbols) bands relative to that of the α_1 band for [S#1 (1.96), S#1 (1.58), and S#2 (1.96)]. Symbols are described in the legend.

IV. CONCLUSIONS

The phonon Raman scattering in UO_2 was investigated at room temperatures under pressures up to 29 GPa with an excitation energy range of $E_i=1.16$-2.41 eV. At ambient pressure up to six-order polarized multi LO-phonon bands are detected with a resonant profile that follows the UO_2 absorption (threshold of ~2.0 eV). The resonance profile of the 1–6 LO intensities is likely to be attributed to "forbidden" Fröhlich LO(Γ) scattering. However, the identification with this form of scattering cannot explain the different polarization sensitivity between the even (strongly polarized) and odd (weakly polarized) bands. Hence, significant contribution of nearly degenerate disorder-induced phonons extending over the Brillouin zone from Γ to L boundaries[5] is suggested.

The 1150 cm^{-1} band found by Schoenes[2] is reassigned to the 2 LO band rather than to the Γ_5-Γ_3 crystal field electronic transition. This assignment is supported by the similarity with the 576 cm^{-1} (1 LO) bands in the resonance profile, Grüneisen parameters, and the dependence of the intensity profiles on pressure. The previous assignment of the 1150 cm^{-1} band to the CF transition was mostly due to the accepted notion that a decrease in intensity with temperature

is not expected from pure multiphonon excitation but rather from a band of electronic origin. Correlating our result with YbS,[32] that are characterized by $4f$ localization, suggests that lifetime effects of the excited electronic state are responsible for the observed decrease with the temperature in the 2 LO intensity.[2,12]

The increase in pressure is accompanied by (i) A redshift in the resonance onset of the 1 LO and 2 LO bands that is related to the decreasing band gap, (ii) an increase in the electron-phonon interactions strength that leads to their increased intensities, and (iii) decreasing the incident and scattered light penetration depth, due to the increased absorption. For $E_i = 1.96$ eV, the interplay between these factors result in the increase of the 1 LO and 2 LO bands intensities up to ~10 GPa that is followed by a decrease at higher pressures.

ACKNOWLEDGMENTS

We thank Dr. Arye Tishbee from the Weizmann Institute of Science for enabling the usage of the Renishaw dispersive and Bruker FT-Raman spectrometers and to Professor Moshe Mintz for providing the UO_2 pellets. We gratefully acknowledge Professor K. Syassen for sending us his unpublished manuscript with pressure dependent UO_2 reflectivity data and Dr. Ilan Yaar for providing us with preliminary results on pressure dependent electronic DOS calculations.

*Corresponding author. Email address: T.Livneh@nrcn.org.il

[1] J. Schoenes, Phys. Rep. **63**, 301(1980).
[2] J. Schoenes, J. Chem. Soc., Faraday Trans. 2, **83**, 1205 (1987).
[3] I. S. Butler, G. C. Allen, and N. A. Tuan, J. Nucl. Mater. **144**, 17 (1987).
[4] P. R. Graves, Appl. Spectrosc. **44**, 1665 (1990).
[5] G. Dolling, R. A. Cowley, and A. D. B. Woods, Can. J. Phys. **43**, 1397 (1965).
[6] H. U. Rahman and W. A. Runciman, J. Phys. Chem. Solids **27**, 1833 (1966).
[7] S. Kern, C.-K. Loong, and G. H. Lander, Phys. Rev. B **32**, 3051 (1985).
[8] R. Osborn, A. D. Taylor, Z. A. Bowden, M. A. Hackett, W. Hayes, M. T. Hutchings, G. Amoretti, R. Caciuffo, A. Blaise, and F. Fournier, J. Phys. C **21**, 1931 (1988).
[9] G. Amoretti, A. Blaise, R. Caciuffo, J. M. Fournier, M. T. Hutchings, R. Osborn, and A. D. Taylor, Phys. Rev. B **40**, 1856 (1989).
[10] S. Blumenröder, H. Brenten, E. Zirngiebl, R. Mock, G. Güntherodt, J. D. Thompson, Z. Fisk, and J. Naegele, J. Magn. Magn. Mater. **76/77**, 331 (1988).
[11] M. L. Palacios and S. H. Taylor, Appl. Spectrosc. **54**, 1372 (2000).
[12] D. Manara and B. Renker, J. Nucl. Mater. **321**, 233 (2003).
[13] S. D. Senanayake, R. Rousseau, D. Colegrave, and H. Idriss, J. Nucl. Mater. **342**, 179 (2005).
[14] U. Benedict, G. D. Andreetti, J. M. Fournier, and A. Waintal, J. Phys. (Paris) **43**, L–171 (1982).
[15] K. Syassen, H. Winzen, and U. Benedict, Physica B & C, **144**, 91 (1986)
[16] K. Syassen, H. Winzen, P. J. Kelly, M. S. S. Brooks, and U. Benedict (unpublished).
[17] U. Benedict, J. Alloys Compd. **213/214**, 153 (1994).
[18] T. M. Benjamin, G. Zou, H. K. Mao, and P. M. Bell, Annual Report 1980–1981, Geophysical Lab., Washington DC.
[19] M. C. Pujo, M. Idri, L. Havela, S. Heathman, and J. Spino, J. Nucl. Mater. **324**, 189 (2004).
[20] M. Idri, L. T. Le Bihan, S. Heathman, and J. Rabizant, Phys. Rev. B **70**, 014113 (2004).
[21] S. T. Duclos, Y. K. Vohra, A. L. Ruoff, A. Jjayaraman, and G. P. Espinosa, Phys. Rev. B **38**, 7755 (1988).
[22] J. Staun Olsen, L. Ggerward, V. Kanchana, and G. Vvaitheeswaran, J. Alloys Compd. **381**, 37 (2004).
[23] P. J. Kelly and M. S. S. Brooks, J. Chem. Soc., Faraday Trans. 2 **83**, 1189 (1987).
[24] W. H. Weber, K. C. Hass, and J. R. McBride, Phys. Rev. B **48**, 178 (1993).
[25] G. A. Kourouklis, A. Jayaraman, and G. P. Espinosa, Phys. Rev. B **37**, 4250 (1988).
[26] M. Iishgame and M. Kojima, J. Phys. Soc. Jpn. **41**, 202 (1976).
[27] A. Jayaraman, G. A. Kourouklis, and L. G. Van Uitert, Pramana **30**, 225 (1988).
[28] J. M. Cassado, J. M. Harding, and G. J. Hyland, J. Phys.: Condens. Matter **6**, 4685 (1994).
[29] G. J. Hyland, J. Nucl. Mater. **113**, 125 (1983).
[30] P. Ruello, R. D. Becker, K. Ullrich, L. Desgranges, C. Petot, and G. Petot-Ervas, J. Nucl. Mater. **328**, 46 (2004).
[31] M. Cardona, in *Light Scattering in Solids II*, edited by M. Cardona and G. Güntherodt, Topics in Applied Physics, Vol. 50 (Springer-Verlag, Berlin, 1982). p.19.
[32] R. Merlin, G. Güntherodt, R. Humphreys, M. Cardona, R. Suryanarayanan, and F. Holtzberg, Phys. Rev. B **17**, 4951 (1978).
[33] T. R. Griffiths and H. V. St. A. Hubbard, J. Nucl. Mater. **185**, 243 (1991).
[34] K. N. Kudin, G. E. Scuseria, and R. L. Martin, Phys. Rev. Lett. **89**, 266402 (2002).
[35] L. E. Cox, W. P. Ellis, R. D. Cowan, J. W. Allen, S.-J. Oh, L. Lindu, B. B Pate, and A. J. Arco, Phys. Rev. B **35**, 5761 (1987).
[36] M. Mintz, S. Vaknin, A. Kremner, and Z. Hadari, NRCN Report No. 435, 1977.
[37] E. Sterer, M. P. Pasternak, and R. D. Tailor, Rev. Sci. Instrum. **63**, 1117 (1991).
[38] Mao H. K., Xu J., and Bell P. M,. J. Geophys. Res. **91B**, 4673 (1986).
[39] T. Livneh, (unpublished)
[40] The γ for α_3^3-α_3^6 were not detected due to the overlapping with the electronic-phononic Raman bands [β bands (Ref. 39)], the intense first order diamond band (α_3^3), second order diamond band (α_3^4), or very poor signal-to-noise ratio (α_3^5, α_3^6).
[41] L. Gerward, J. Staun Olsen, L. Petit, G. Vaitheeswaran, V. Kanchana, and A. Svane, J. Alloys Compd. **400**, 56 (2005).
[42] S. S. Mirta, O. Brafman, W. B. Daniels, and R. K. Crawford, Phys. Rev. **186**, 942 (1969).
[43] R. Ruppin, J. Phys. Chem. Solids **33**, 83 (1972).

[44] B. A. Weinstein and R. Zallen, in *Light Scattering in Solids IV*, edited by M. Cardona and G. Guntherodt, Topics in Applied Physics Vol. 54 (Springer-Verlag, Berlin, 1984) p. 463.
[45] L. Tribe, R. M. Fracchia, J. A. O. Bruno, and A. Batana, Comput. Chem. (Oxford) **19**, 403 (1995).
[46] G. C. Allen and P. A. Tempest, J. Chem. Soc. Dalton Trans. **1983**, 2673.
[47] J. Schoenes, J. Phys. C **5**, 31 (1980).
[48] J. Vitin and P. Wachter, Physica B & C **86-88**, 213 (1977).
[49] M. V. Abrashev, A. P. Litvinchuk, C. Thomsen, and V. N. Popov, Phys. Rev. B **55**, R8638 (1997).
[50] G. D. Smith, S. Firth, R. J. H. Clark, and M. Cardona, J. Appl. Phys. **92**, 4375 (2002)
[51] R. M. Martin and T. C. Damen, Phys. Rev. Lett. **26** 86, (1971).
[52] G. Güntherodt, P. Grünberg, E. Anastassakis, M. Cardona, H. Hackfort, and W. Zinn, Phys. Rev. B **16**, 3504 (1977).
[53] J. C. Tsang, M. S. Dresselhaus, R. L. Aggarwal, and T. B. Reed, Phys. Rev. B **9**, 984 (1974).
[54] J. G. Conway, J. Chem. Phys. **31**, 1002 (1959).